Two-Dimensional Simulation Model for Contour Basin Layouts in Southeast Australia. II: Irregular Shape and Multiple Basins

Manoj Khanna[1]; Hector M. Malano, A.M.ASCE[2]; John D. Fenton[3]; and Hugh Turral[4]

Abstract: The development of a two-dimensional simulation model for single regular shape (rectangular) contour basin irrigation layout in southeast Australia is reported in a companion paper. Contour basin layouts as used in Southeast Australia are often irregular in shape and laid out as multiple basin systems. Irrigation of these basins is carried out sequentially involving back flow to the supply channel and inter-basin flow. This paper presents the extension of the earlier model to incorporate irregular shape basins and multiple basin operation. The governing equation is solved by adopting a ''split-operator approach'' using the method of characteristics coupled with two-dimensional Taylor series expansion for interpolation and calculation of diffusion terms. The numerical solution scheme is based on a grid of quadrilaterals for spatial discretization, to provide geometric flexibility. Infiltration is computed using either the empirical Kostiakov–Lewis equation or the quasianalytical Parlange equation. The model was validated against field data collected from irrigation events monitored on a commercial laser leveled contour layout consisting of five basins.

DOI: 10.1061/(ASCE)0733-9437(2003)129:5(317)

CE Database subject headings: Two-dimensional flow; Simulation models; Australia; Basins; Irrigation.

Introduction

Contour basin irrigation layouts are used in Australia for cultivation of rice on soils with low infiltration rates. The banks of the contour basins are erected across the slope, following the contour of the land. These banks are built by borrowing soil from the outside edges of the bank. The resulting borrow pit or toe-furrow serves as a supply channel as well as a drainage channel for the basin. The water supply channels are constructed down slope in order to provide a direct water supply to each basin over the entire length of the basin inlet.

Irrigation of these layouts is carried out progressively from the first basin to the bottom basin. Fig. 1 shows a typical flow pattern during the inflow-advance phase and Fig. 2 shows a typical flow pattern during recession-drainage phase. Water is allowed to flow into the basin until the entire basin is flooded at which time the inflow is cut off and water is allowed to drain back into the supply channel and into the downstream basin through gaps in the check bank. At the same time, supply is cut off from the first basin and diverted towards the second basin. While water is supplied to the second basin, the surplus water from the first basin is also allowed to drain into the second basin through gaps in the check bank as well as back into the supply channel. When the second basin is completely irrigated, water supply is diverted to the third basin and so on until all the basins in the irrigation block are fully irrigated. Drainage runoff from the last basin in a sequence may be diverted into storage for recycling. Normally 5–10 basins of different sizes and shapes are included in an irrigation block.

A two-dimensional simulation model for single regular shape rectangular basins, is presented in a companion paper by Khanna et al. (2003), which we refer to as Paper I. The model is based on a single two-dimensional advection-diffusion equation including infiltration as a sink. Infiltration can be modeled by either the empirical Kostiakov–Lewis equation (Clemmens et al. 1981; Playan et al. 1994a,b) or the quasianalytical Parlange equation (Haverkamp et al. 1990). The advection–diffusion equation was solved by adopting a ''split-operator approach'' (Holly and Preissmann 1977; Glass and Rodi 1982; Holly and Usseglio-Polatera 1984; Holly and Toda 1985; Komatsu et al. 1985; Komatsu et al. 1997) using the method of characteristics coupled with bicubic splines for interpolation and calculation of the diffusion components. The numerical solution methodology was based on a rectangular grid for spatial discretization.

In this paper, the same model was extended to irregular shape basins and multiple basin systems which are typical of contour layouts used in Southeast Australia. This extended model is based on the same governing equation which is solved on a grid of quadrilateral discretisation that incorporates the geometrical flexibility needed for irregular basins. The model also incorporates both the empirical Kostiakov–Lewis infiltration model and the quasi-analytical Parlange infiltration model (Khanna et al. 2003) to describe the infiltration process. It must be noted here that this type of discretisation can also be used for regular shape rectan-

[1]Senior Scientist, Water Technology Centre, Indian Agricultural Research Institute, New Delhi 110012, India. E-mail: mkhanna@iari.res.in

[2]Associate Professor, Dept. of Civil & Environmental Engineering, University of Melbourne, Victoria 3010, Australia. E-mail: h.malano@devtech.unimelb.edu.au

[3]Professor, Dept. of Civil & Environmental Engineering, Univ. of Melbourne, Victoria 3010, Australia. E-mail: fenton@unimelb.edu.au

[4]Senior Researcher, International Water Management Institute, P.O. Box 2075, Colombo, Sri Lanka. E-mail: h.turral@cgiar.org

Note. Discussion open until March 1, 2004. Separate discussions must be submitted for individual papers. To extend the closing date by one month, a written request must be filed with the ASCE Managing Editor. The manuscript for this paper was submitted for review and possible publication on November 27, 2001; approved on January 2, 2003. This paper is part of the ***Journal of Irrigation and Drainage Engineering***, Vol. 129, No. 5, October 1, 2003. ©ASCE, ISSN 0733-9437/2003/5-317–325/$18.00.

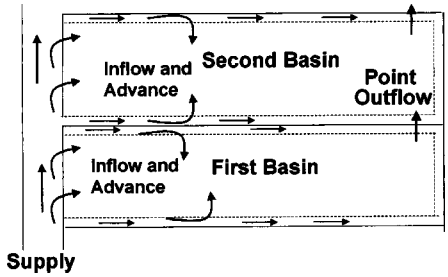

Fig. 1. Water flow patterns in contour basin layouts during inflow and advance

gular basins, as this is only a special case of irregular shape basins.

Numerical Scheme Using Taylor Discretization for Irregular Grids

The solution of this flow problem requires a numerical scheme that offers the maximum geometrical flexibility to accommodate the irregular shape of the computational domain. Overlaying the physical domain with a rectangular computational mesh is not recommended for two reasons: First, it imposes a higher computational overhead; and second the boundary will have to be approximated by a staircase-like boundary curve (Karpik and Crockett 1997). For these reasons, it is desirable to use a numerical scheme that approximates more precisely the boundaries of irregular shape domain and which does not lead to redundant computational nodes that result from the irregular shape of the domain boundary.

Typically, finite element models discretize a complex geometry into sets of triangular elements, but codes based on such a mesh require the use of a complex data structure and are complicated to implement. Also, the transformation of a complex physical geometry into a rectangular computational domain requires a more complex programming effort. A simpler approach is to use a two-dimensional Taylor series expansion (Korn and Korn 1961) about the nodal points in the computational domain to estimate the internodal values of a function defined by its values at the nodes. The coefficients of the series for these nodes are then considered to be unknowns. Discrepancy between the values resulting from Taylor expansion about distinct nodes is allowed if it is of the same order of magnitude as the estimated error resulting from the discretisation. This enables considerable savings in computational effort by avoiding the need to fit the local expansions with a discrepancy smaller than the error that is expected for a

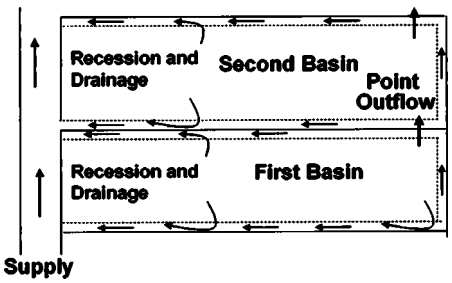

Fig. 2. Water flow patterns in contour basin layouts during recession and drainage

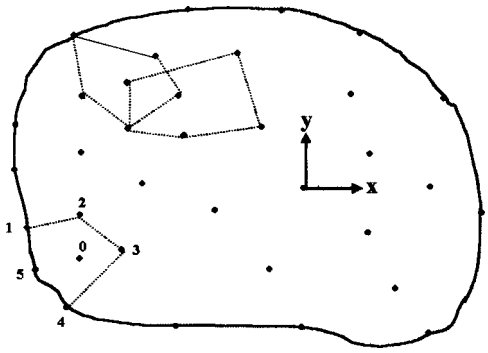

Fig. 3. Discretization of irregular shape domain

given grid size and order of expansion (Kochavi et al. 1991). This method offers good geometrical flexibility by allowing the user to choose the location of the nodal points and vary the distance between them. The Taylor series method requires continuity at each node. This, however, is unlikely to be a problem since the governing differential equations are always continuous (Sonnemans et al. 1991). The number of neighboring nodes checked for continuity depends only on the order of the polynomial representing the dependent variable in the vicinity of each node. There are no other restrictions and in principle the location and numbering order of neighboring nodes is not important. Moreover, the computational effort is not influenced by the order of numbering of the nodes (Kochavi et al. 1991). This method has been used by several researchers for the solution of ordinary differential equations (Sonnemans et al. 1991) and for the solution of nonlinear heat transfer problems (Kochavi et al. 1991; Kochavi et al. 1993).

The numerical solution of a single advection–diffusion equation based on the ''split-operator approach'' including infiltration as a sink was used to describe overland flow in rectangular contour basin irrigation layouts in Paper I (Khanna et al. 2003). The numerical scheme proposed in this study also uses a ''split-operator approach'' for the solution of the governing equation. A two-dimensional Taylor discretisation scheme is used to compute the advection and diffusion components of the governing equation. The concept behind the numerical scheme is described in Fig. 3. The figure shows a hypothetical distribution of computational points (shown as dots) and the overlapping of computational polygons. In addition, a computational subdomain consisting of a central node surrounded by five nodal points is also described.

Consider point 0 and five neighboring points 1,2, . . . ,5, which outline the boundaries of a local region around it. By introducing a local two-dimensional Taylor series about point 0 for the function H representing water surface elevation, the value of H at any point can be represented as

$$H = H_0 + x\frac{\partial H}{\partial x} + y\frac{\partial H}{\partial y} + \frac{1}{2!}\left(x^2\frac{\partial^2 H}{\partial x^2} + 2xy\frac{\partial^2 H}{\partial x \partial y} + y^2\frac{\partial^2 H}{\partial y^2}\right) + \cdots \quad (1)$$

where in the right hand side values of H and its derivatives are at the reference point 0, and the x and y are local coordinates, relative to (0,0) which denote the reference point. At the reference point, the trivial solution is $H = H_0$. It follows that the solution of Eq. (1) at any other point i in the vicinity with coordinates (x_i, y_i) after rearranging becomes

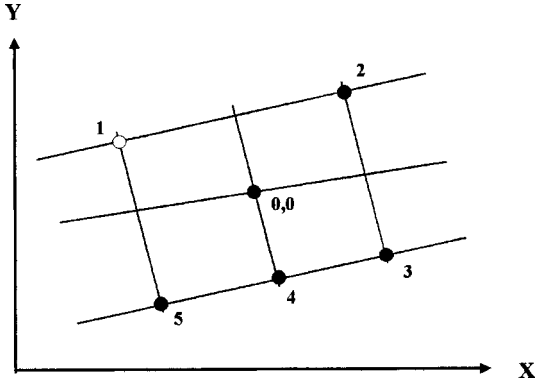

Fig. 4. Location of surrounding points for interior nodes

$$(x_i-x_0)\frac{\partial H}{\partial x}+(y_i-y_0)\frac{\partial H}{\partial y}+\frac{1}{2}(x_i-x_0)^2\frac{\partial^2 H}{\partial x^2}+(x_i-x_0)$$

$$\times(y_i-y_0)\frac{\partial^2 H}{\partial x\partial y}+\frac{1}{2}(y_i-y_0)^2\frac{\partial^2 H}{\partial y^2}=H_i-H_0 \quad (2)$$

Taking five such equations at five points (1,2, . . . ,5) surrounding point 0 with given x_i, y_i, H_i will yield a system of equations which can be solved for the five unknowns

$$\frac{\partial H}{\partial x};\quad \frac{\partial H}{\partial y};\quad \frac{\partial^2 H}{\partial x^2};\quad \frac{\partial^2 H}{\partial y^2};\quad \frac{\partial^2 H}{\partial x\,\partial y}$$

at point 0. There are no restrictions on the relative position of the neighboring nodes; however, it is preferable that they be selected from the nearest vicinity of the central node. In particular, points on the boundary should be selected for central nodes that are located near the boundary. The points are used in the calculation of the function and derivatives at neighboring internal nodes, but no polynomial approximation is calculated for boundary nodes themselves. For interior nodes, the location of surrounding points (1,2, . . . ,5) is shown in Fig. 4.

This system of equations is solved using the process of lower triangular matrix-upper triangular matrix (LU) decomposition (Press et al. 1989) to determine the unknown coefficients. In principle, having five equations for each nodal point and N nodes arbitrarily distributed in the domain including boundary nodes allows a $5N\times 5N$ global system of equations to be written and solved for $5N$ unknown coefficients. The set of five equations in matrix form can be written as

$$[H_i-H_0]=[X]\cdot[A] \quad (3)$$

where $[H_i-H_0]$=column vector of dimension 5 that contains the known values of the function at surrounding nodes; $[X]$=matrix of order 5×5; and $[A]$=five-column vector that contains five unknown coefficients, representing the values of first, second and mixed derivatives of the function H at the node (0,0). Eq. (3) can be solved efficiently using the LU decomposition method for the unknown coefficients. This solution gives the value of first, second, and mixed derivative of H at the central node (0,0). The first derivatives of H are then used to calculate the advected velocities in the x and y directions.

The solution of the advected component of the governing equation, at a new time step, is given by the characteristic equation (Khanna et al. 2003). The location and interpolated value of H at the point is determined by using a Taylor series discretization. The interpolated value of H incorporating Taylor series is given by

$$H^*(x_i,y_j,t+\Delta)=H(x_i-U_{i,j}\Delta,y_j-V_{i,j}\Delta,t)$$

$$=H_{0,0}+(-U\Delta)\left.\frac{\partial H}{\partial x}\right|_{0,0}+(-V\Delta)\left.\frac{\partial H}{\partial y}\right|_{0,0}$$

$$+\frac{1}{2}(-U\Delta)^2\left.\frac{\partial^2 H}{\partial x^2}\right|_{0,0}+(-U\Delta)$$

$$\times(-V\Delta)\left.\frac{\partial^2 H}{\partial x\partial y}\right|_{0,0}+\frac{1}{2}(-V\Delta)^2\left.\frac{\partial^2 H}{\partial y^2}\right|_{0,0} \quad (4)$$

where U and V=advected velocities (Khanna et al. 2003); t=time (s); and Δ=time step.

For the computation of the diffusion component, the value of the second and mixed derivative of H at the interpolated point is required. The second and mixed derivatives of H at interpolated points are assumed the same as at the central node (0,0). These derivatives are already available from the solution of the system of equations given by Eq. (3). Thus, the final solution of H at the next time step will be given by the combined equation (Khanna et al. 2003), which incorporates the advection, diffusion, and infiltration terms.

The elevation gradients at the nodal points in the x and y directions are required to be estimated for the computation of advection velocities. The methodology based on Taylor series discretisation is used to compute the elevation gradients at nodal points on an irregular grid from observed elevation data at five surrounding nodes which yields a set of five equations using Eq. (2). The elevation gradients at nodal points are determined by solving the system of equations given by Eq. (3) using LU decomposition (Press et al. 1989).

Initial and Boundary Conditions (Multiple Basin Systems)

The methodology used to implement the numerical solution is explicit in nature requiring a set of initial and boundary conditions. At $t=0$ the land surface elevation $z_0(x,y)$ is an initial condition and an input to the model. Infiltration depth at $t=0$ is set to zero at all nodes. The entire computational boundary is divided into two types of boundary conditions: Inflow boundary and outflow boundaries. In addition, an internal boundary condition (Khanna et al. 2003) was also imposed to overcome the problem arising due to a node which is characterized by a bottom elevation higher than the water surface elevation in a neighboring node. In such a case, water would flow outward from the dry node which is a physical impossibility.

Inflow Boundary

In a multiple basin system, inflow boundary conditions (line-inflow) are imposed to the first basin to simulate inflow from the supply channel. The water surface elevation in the supply channel is imposed as a boundary condition on the inflow side of the basin. The flow depth in toe-furrows derived from the solution of the one-dimensional flow equation (Khanna et al. 2003) is applied as a boundary condition on flow nodes along the toe-furrows. A

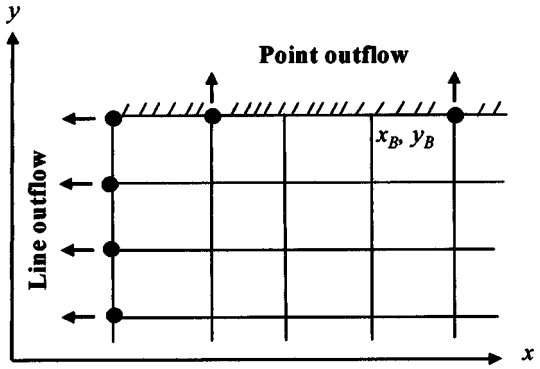

Fig. 5. Outflow boundary

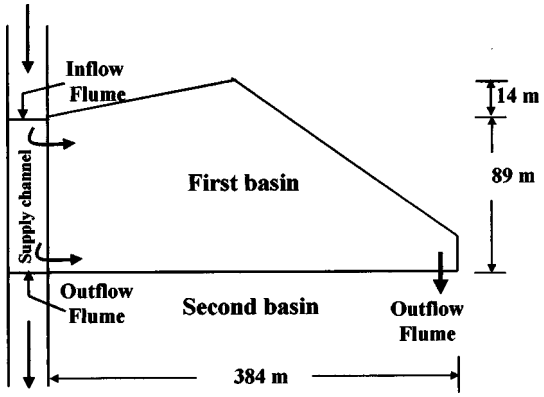

Fig. 6. Layout of single irregular shape contour basin

check is provided in the model to determine whether the upstream first basin is completely filled before the supply to the basin is cut off The model allows two options to specify the cut off time to reflect what normally occurs in practice: (1) user-specified cut off time and (2) inflow cut off on completion of the advance phase. In the first case, if cut off time occurs before advance in the first basin is completed, inflow to the first basin is cutoff and water is allowed to flow into the next basin downstream. The computation then proceeds simultaneously over both basins. In the second case, if cut off occurs on completion of the advance phase, inflow to the upstream basin ceases at this point and inflow from the supply channel and drainage through the check banks into the downstream basin is allowed to start. As in the previous case, the computation continues simultaneously over both basins. A similar process is applied if simultaneous irrigation occurs over additional basins

Point inflows are applied as boundary conditions representing the drainage runoff from the upstream basin in the second and subsequent downstream basins. The node number in the downstream basin specifies the location of point inflow. The location of the node is the same as the outflow node from the upstream basin. The outflow discharge from the first basin becomes the inflow to the second basin. The depth of flow at that node is determined by the simulation in the first basin and imposed as an inflow boundary condition on the downstream basin. The boundary condition for point inflow is then specified as depth of flow as follows:

$$H_{(2)}(x_B,y_B,t)=h_{(1)}(x_B,y_B,t)+z_{0_{(2)}}(x_B,y_B,t) \qquad (5)$$

where $H_{(2)}(x_B,y_B,t)$=water surface elevation at the point inflow node in the downstream basin; $h_{(1)}(x_B,y_B,t)$=depth of flow at the corresponding point outflow node in the upstream basin; $z_{0_{(2)}}(x_B,y_B,t)$=bed elevation at the point inflow node in the downstream basin; and x_B and y_B=values of x and y that define the location of these points on the check bank. All inflow nodes included in the system of equations are solved by the Taylor discretisation scheme described earlier.

Outflow Boundary

During the recession phase after the supply to the upstream basin is cut off, excess water drains from the basin back into the supply channel as well as from a few other points on the check bank into the downstream basin (Fig. 5).

The backflow into the supply channel is termed line-outflow since it occurs along the full length of the basin inlet. The amount and rate of outflow to the supply channel depends on the depth of flow in the supply channel. The boundary condition for this line-outflow is given as the flow depth in the supply channel after the supply to the basin is cut off and drainage outflow into the supply channel starts. This boundary condition is imposed on all the nodes along the supply channel.

Outflow through the check bank into the downstream basin is termed point outflow (drainage runoff) and typically occurs at one or more points along the check bank of the basin (Fig. 5) in a multiple basin operation. Outflow from the basin is triggered by the time of completion of irrigation in the upstream basin and the start of irrigation in the second basin.

The rate of outflow depends on the elevation and flow depth at the corresponding nodes in the upstream and downstream basins. The boundary condition for point outflow is given as the flow depth at the outflow node in the upstream basin. This is expressed as

$$H_{(1)}(x_B,y_B,t)=h_{(2)}(x_B,y_B,t)+z_{0_{(1)}}(x_B,y_B,t) \qquad (6)$$

where $H_{(1)}(x_B,y_B,t)$=water surface elevation at the point outflow node in the upstream basin; $h_{(2)}(x_B,y_B,t)$=depth of flow at the corresponding point inflow node in the downstream basin; $z_{0_{(1)}}(x_B,y_B,t)$=bed elevation at the point outflow node in the upstream basin; and x_B and y_B=values of x and y that define the location of these points on the check bank.

Model Validation

The model was validated for a single irregular shape basin and for two-basin multiple basin operating system incorporating all the

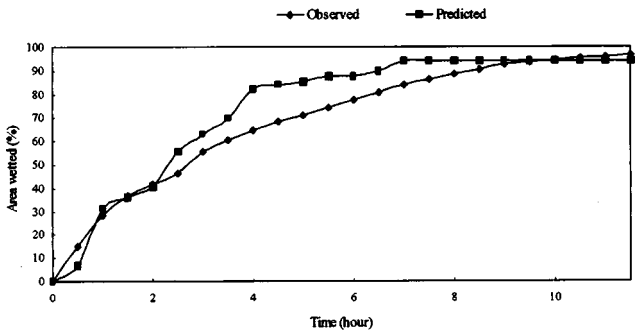

Fig. 7. Waterfront advance trajectory for single irregular shape contour basin with line inflow

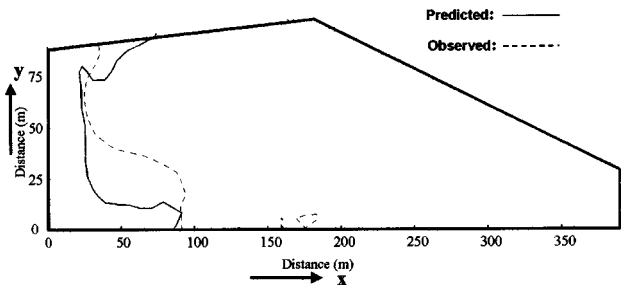

Fig. 8. Waterfront configuration after 30 min in first basin during first irrigation

typical features of this type of layouts. The data used for the validation of the basin model was collected from field experiments conducted during the irrigation season 1999–2000 at Wyanda, New South Wales, Australia. The layout of the field trial and the location of measuring flumes fitted with flow meter are shown in Fig. 6. Data for model validation was collected by monitoring two irrigation events on commercially laser leveled farmer's fields. Field and grid nodes were mapped using a global positioning system (GPS). The GPS was also used to monitor the advance of the waterfront over the field by an operator regularly walking along the advancing waterfront. Additional soil data on surface irrigation parameters were collected from the studies previously conducted on similar soil types. The variables used for model validation were cumulative wetted area, waterfront advance and basin water balance. As indicated above, the model can handle infiltration using either the Kostiakov–Lewis infiltration equation or the Parlange infiltration equation (Khanna et al. 2003). For the purpose of validating the performance of the model for irregular shape basins, only the Kostiakov–Lewis equation was used. Performance of the model to handle Parlange infiltration equation was demonstrated in a companion paper (Khanna et al. 2003).

Model Validation for Single Irregular Shape Basin

Data collected during the first irrigation of the season from the first basin, which is of irregular shape was used for validation of the model. The basin had been laser levelled in both directions about five years earlier although still has local undulations due to movement of sheep and vehicles. The field was currently sown to subclover at the time of the experiment.

The basin was irrigated from the supply channel with an average discharge rate of 0.1 m^3/s for 11.5 h, after which the supply

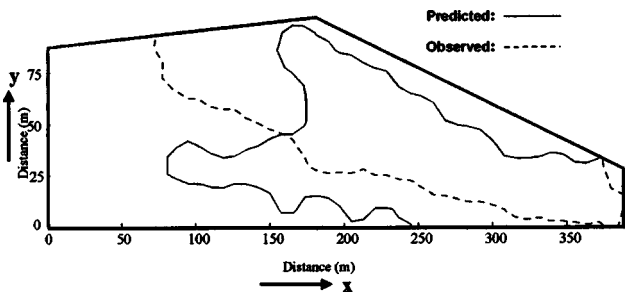

Fig. 9. Waterfront configuration in first basin after 2 h during first irrigation

Table 1. Comparison of Final Water Balance Components in First Basin

	First basin		
Water balance component	Observed (ML)	Predicted (ML)	Error (%)
Inflow volume	4.27	3.85	10
Outflow volume	2.52	2.19	13
Infiltrated volume	1.27	1.18	7
Evaporation	0.48	0.48	—

was cut off and diverted to the second basin downstream. Infiltration was described by the Kostiakov–Lewis equation and its parameters taken as $k=0.055\ \text{m/s}^{0.026}$; $a=0.026$; and $b=0.0\ \text{m/s}$ (Maheshwari and Jayawardane 1992; Hume 1993). Manning's coefficient was taken as 0.29 (Maheshwari and McMahon 1992) and the field was completely dry and the soil was heavily cracked. The contour basin was discretized in a 12.5 and 12.8 m grid in x and y directions respectively yielding a total of 256 nodes, 32 in the x direction and 8 in the y direction. The soil surface elevations used in the simulation were measured on a grid size of 12.5×12.8 m in the field. The simulation model was run for total time of simulation of 49 h.

Advance Phase

Cumulative Wetted Area During Advance

Fig. 7 shows the comparison between observed wetted area during the advance phase and wetted area predicted by the model. The predicted results shown in Fig. 7 satisfactorily match the observed values indicating that the model is capable of simulating advance wetted area in basins of irregular shape. The maximum deviation between observed and modeled advanced area which occurs in the middle range of the advance trajectory between 4 and 8 h is 17% of the measured values. This variation between may be due to variation in local topography, soil characteristics and inflow rates. Despite some departure between measured and modeled values during the advance phase, good agreement is observed in the final stages of the irrigation event when most of the basin area has been covered.

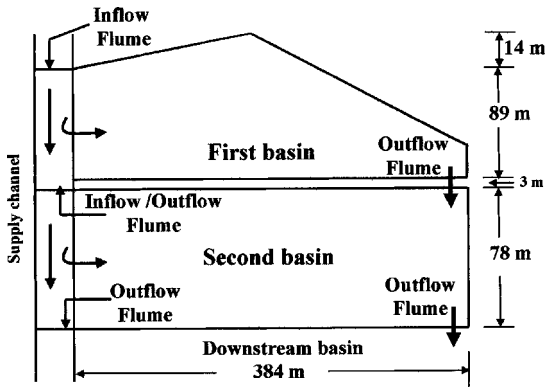

Fig. 10. Layout of multiple basins for validation

Table 2. Values of Model Parameters Used for Simulation

Basin	Line inflow (m^3/s)	Time of irrigation (h)	Drainage inflow (m^3/s)	Number of nodes	Manning's roughness coefficient n	Infiltration parameters		
						k (m/s^a)	a	b (m/s)
First	0.1	9	—	256	0.17	0.037	0.03	0.0
Second	0.12	6	0.025	224	0.17	0.037	0.021	0.0

Waterfront Advance Pattern

Figs. 8 and 9 show the comparison of the waterfront advance pattern as observed and predicted by the model after 30 min and 2 h of advance time. The results predicted by the model compare reasonably well with the observed waterfront pattern. All deviation are within 17% of the observed advance distance. On the basis of this comparison, the model exhibits a good capability to simulate advance considering that the spatial variability of infiltration and local microtopography are not considered at this scale of modeling.

Prediction of waterfront advance along the toe-furrows is very close to actual advance. In this type of basin layouts, the toe-furrows get filled first subsequently allowing the water to move inward. This behavior is depicted in Figs. 8 and 9 where the waterfront in the toe furrow is moving ahead of waterfront in the center of the basin.

Basin Water Balance

The water balance predicted by the model after the completion of the irrigation event was compared with the field measured volume balance. The water balance quantities predicted by the model are inflow, outflow, and infiltration volume. The observed infiltration volume was determined by taking pre- and postirrigation moisture measurements adjusted by evaporation obtained from direct measurement during the experiment. The water balance components are shown in Table 1.

The errors in the predicted water balance components were 10% for inflow, 13% for outflow, and 7% for infiltration. Similarly to other validation variables, the possible reasons for the minor deviation observed are local undulations, and spatial variability of infiltration which are not accounted within the level of resolution adopted in the model for these variables.

Validation for Multiple Basin Systems

The simulation model for irregular shape contour basins was also validated for an extended system that incorporates multiple basins. The objective of this validation is to evaluate the simulation model that incorporates all the key geometric features of multiple contour basin layouts as practiced in southeast Australia.

Data collected during the field experiments conducted during the second irrigation of season 1999–2000 at Wyanda, New South Wales, Australia was used for validation of the model. In this irrigation, the first basin was supplied from the head channel along the entire length of the inlet (line inflow) while the second basin was supplied from the head channel and drainage runoff from the first basin. The layout, dimensions of the two basins and the location of different flumes with flow meter are shown in Fig. 10. Inflows and outflows were measured by flumes fitted with flow meters which were installed in the supply channel to measure basin inflow (line inflow boundary) and basin outflow, and in the check bank to measure drainage outflow through the check bank (point inflow to downstream basin). Both basins had been laser levelled in both directions about 5 years earlier although they still have local undulations due to movement of sheep and vehicles. The basins were sown to sub-clover at the time of the experiment.

The set of basins shown in Fig. 10 comprises one basin of irregular shape and one basin of rectangular shape. The first basin was first irrigated from the supply channel (line inflow); after which the supply was then cutoff and diverted to the second basin downstream. During this time, the inflow to the second basin included both the normal flow in the supply channel plus the drainage backflow from the first basin. In addition, the second basin received drainage outflow from the first basin through gates in the check bank.

A lower value of Manning's roughness coefficient was used for both basins compared to the first irrigation. At the time of the second irrigation, the soil was relatively wet and all the cracks were closed. Prior research carried out by Maheshwari and McMahon (1992) shows a similar change in the roughness coefficient under this soil condition. Different infiltration parameters were used for the first and second basin to test the capability of model to handle varying parameters for different basins. The values of all these parameters used for the model simulation for both the basins are shown in Table 2. Infiltration parameters for the Kostiakov–Lewis equation were taken from studies conducted on

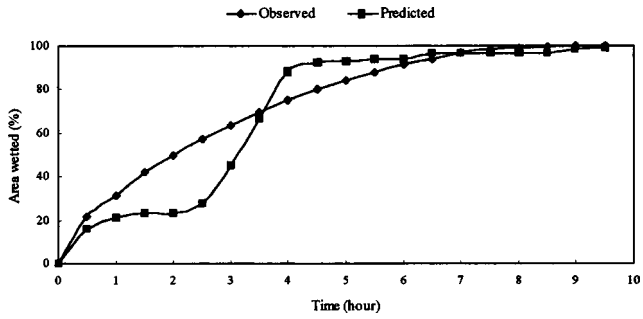

Fig. 11. Comparison of wetted area during advance for first basin

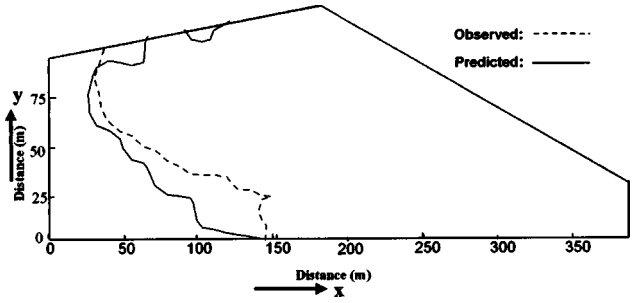

Fig. 12. Waterfront advance pattern after 30 min in first basin

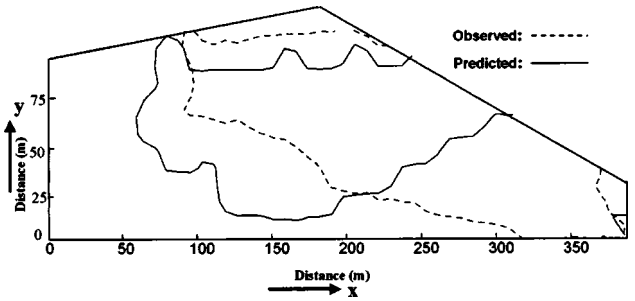

Fig. 13. Waterfront advance pattern after 2 h in first basin

the similar type of soils in the area (Maheshwari and Jayawardane 1992; Hume 1993). The ground elevation of both basins was surveyed on a grid spacing of 12.5×12.8 m which was also used for discretisation of the computational grid.

Cumulative Wetted Area During Advance (First Basin)

Fig. 11 shows the comparison of observed and predicted wetted area during advance phase in the first basin. The figure indicates that the observed and modeled wetted area differ slightly during the initial period of advance but matches satisfactorily the second half of the irrigation period.

The deviation in the prediction of wetted area during the first half of irrigation event was due to the effect of toe-furrows which had been cleaned and deepened at the start of the 1999–2000 season. The simulation model does not allow water onto the nodes adjacent to the toe-furrows until the furrows are completely filled. This approach tends to cause a rapid increase in the wetted area when the toe-furrows have just begun to overflow onto the interior of the basin. This effect is more pronounced in the prediction of wetted area for the simulation of irrigation events in the 1999–00 season. However, once the toe-furrows are completely filled, the predicted and observed wetted area matches very closely.

Waterfront Advance Pattern (First Basin)

Figs. 12 and 13 show the comparison of waterfront advance patterns in the first basin after 30 min and 2 h of elapsed time, respectively. Minor variations in the predicted and observed advance pattern can be attributed to local topographic irregularities which are not captured by the grid size used in the simulation. It is possible that the finer discretisation grid will result in a more accurate waterfront pattern as found in an earlier model validation of rectangular shape basins (Singh 1996). It can also be observed

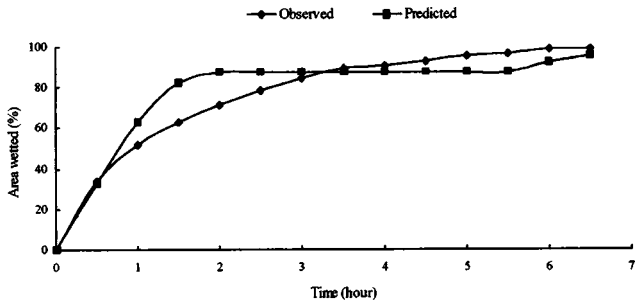

Fig. 14. Comparison of wetted area during advance for second basin

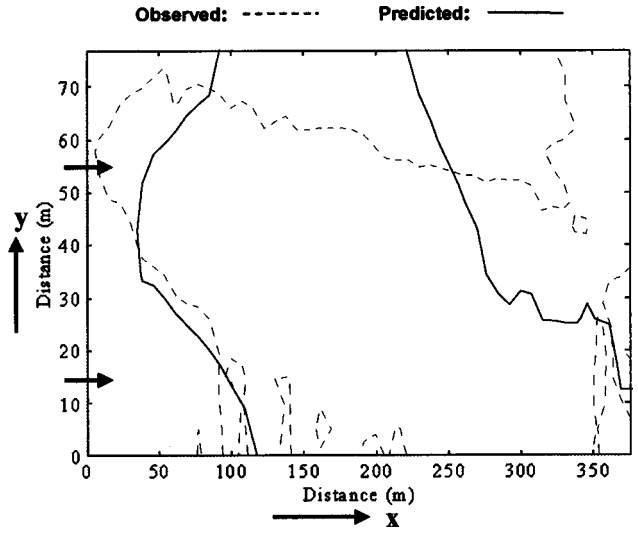

Fig. 15. Waterfront advance pattern in second basin after 30 min (arrows indicate direction of flow)

that the model predicts the cumulative variables with better accuracy that the intermediate values.

Cumulative Area Wetted During Advance (Second Basin)

Upon completion of irrigation of the first basin, water supply was diverted to the second basin from the supply channel together with drainage runoff from the first basin which becomes point inflow for the second basin. This allowed the collection of data for validation of the model under dual inflow boundary conditions: line inflow from the supply channel and point inflow from the upstream basin. Fig. 14 shows the comparison of the cumulative wetted area predicted by the model and observed wetted area during the advance phase for the second basin.

The predicted wetted area during advance matches very closely the observed data for the entire duration of advance phase. The prediction of cumulative wetted area also shows the effect of

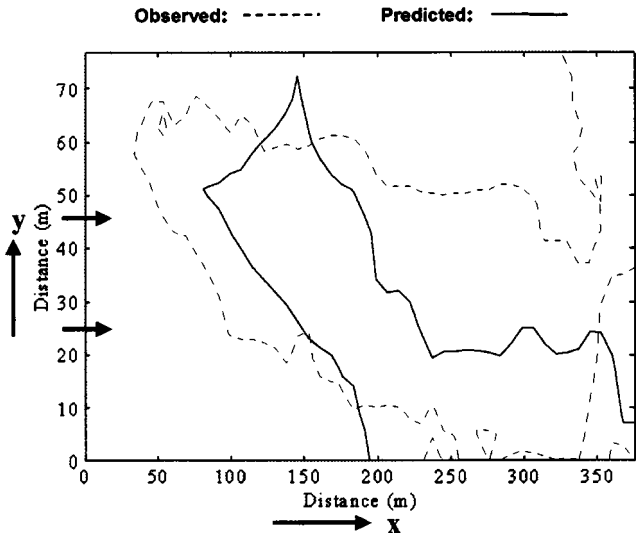

Fig. 16. Waterfront advance in second basin after 1 h (arrows indicate direction of flow)

Table 3. Comparison of Observed and Simulated Water Balance

Parameter	First basin			Second basin		
	Observed (ML)	Predicted (ML)	Error (%)	Observed (ML)	Predicted (ML)	Error (%)
Inflow volume	3.56	3.57	0.2	3.74	2.96	21
Outflow volume	2.23	2.17	3	2.33	1.9	18
Infiltrated volume	1.01	1.08	7	1.11	0.77	30
Evaporation	0.32	0.32	—	0.30	0.30	—

toe-furrows filling whereby the simulated advance is faster shortly after the tow-furrows fill and water begins advancing towards the center of the basin. The final predicted advance however matches the observed advanced very closely.

Waterfront Advance Pattern (Second Basin)

The prediction of waterfront advance was compared periodically with observed data to test the model's capability to incorporate line inflow as well as point inflow in multiple basin scenarios. Figs. 15 and 16 show the comparison of observed and predicted waterfront advance pattern after 30 minute and 1 h, respectively. Time here is measured as the elapsed time from the start of inflow into the second basin. As expected, the observed advance front is more irregular than the model prediction as a result of the surface irregularities in the basin. Nevertheless the computer predicted waterfront depicts the overall advance pattern very accurately.

Overall Water Balance

The final water balance for the irrigation event was computed by simulating the behavior of the composite system comprising the two basins included in the experiment. Table 3 shows the summary of predicted and observed water balance in each basin. Both the predicted and observed quantities were adjusted by the same evaporation amount measured during the field experiment.

The predicted inflow volume for the first basin matches very closely the observed volume of inflow. The error in prediction ranges from 0.2% for the first basin to 21% for the second basin. It should be noted here that the observed volume was based on the average flow measured in the supply channel during the irrigation event. The predicted inflow volume consists of the sum of overland depth and infiltrated depth calculated by the model at the time of shutting off the water supply to the basin.

The comparison of infiltrated volume predicted by the model during the irrigation event shows that the water balance simulation is superior for the first basin than for the second basin. The error in prediction ranges from 7.0% for the first basin to 30% for the second basin. The greater closure error in the second basin can be ascribed in part to less accurate measurement of interbasin drainage runoff due to some leakage during the experiment and to fluctuations in the supply channel discharge during the experiment. Flow fluctuations in the supply channel were not replicated in the model simulation. The outflow volume includes the backflow into the supply channel and the drainage runoff through the check bank into the second basin. In both cases the comparison of outflow volume predicted by the model with the observed values indicates that the model can simulate inter-basin flow with reasonable accuracy.

Conclusions

A two-dimensional mathematical computer simulation model was developed to simulate the hydraulic processes involved in the irrigation of contour basin layouts in southeast Australia. The model is based on the zero-inertia approximation to the shallow water flow equations, leading to a two-dimensional advection–diffusion equation that includes infiltration as a sink term. The model incorporates all the key geometric features of contour layouts and calculates infiltration using either the empirical Kostiakov–Lewis equation or quasianalytical Parlange equation.

The two-dimensional advection–diffusion equation was found to be capable of describing the shallow water flow in contour basin irrigation systems. This single equation was solved by the method of characteristic coupled with a two-dimensional Taylor series expansion for irregular grids. The numerical schemes were found to be accurate, and easy to implement.

The model's capability for simulating irregular shape basins was tested by contrasting predicted and observed results of cumulative advance wetted area, waterfront advance pattern and water balance. These variables were evaluated in a single basin of irregular shape irrigated from the supply channel and a second basin conjunctively supplied from the supply channel and drainage runoff from the upstream basin. While the model can describe infiltration by the Kostiakov–Lewis infiltration and the quasianalytical Parlange equation, all the validation tests were conducted with Kostiakov–Lewis parameters.

The model prediction of cumulative wetted area and waterfront advance compared well with the observed data. The model was also capable of simulating advance of the waterfront including the effect of boundary toe-furrows. The predicted overall basin water balance after the completion of the irrigation event matches the observed values within 7 and 30% for the first basin and second basin, respectively.

Acknowledgment

The writers would like to thank the Land and Water Resources & Development Corporation, Australia for its financial support of this project and the University of Melbourne for providing a student scholarship.

Notation

The following symbols are used in this paper:

a = infiltration empirical constant;
b = infiltration empirical constant;
g = acceleration due to gravity (m/s^2);
H = water surface elevation above datum (m);
h = water depth (m);
k = empirical infiltration constant;
t = time (s);
U = advected velocity in x direction (m/s);
V = advected velocity in y direction (m/s);
x,y = Cartesian coordinates (m);
x_B, y_B = value of x and y on fixed boundary;

z_0 = bottom elevation above datum (m); and
Δ = time step (s).

Subscripts

B = boundary nodes;
i, j = location of node on computation grid; and
x,y = Cartesian coordinates.

References

Clemmmens, A. J., Strelkoff, T., and Dedrick, A. R. (1981). ''Development of solution for level-basin design.'' *J. Irrig. Drain. Eng.*, 107(3), 265–279.

Glass, J., and Rodi, W. (1982). ''A higher order numerical scheme for scalar transport.'' *Comput. Methods Appl. Mech. Eng.*, 31, 337–358.

Haverkamp, R., Parlange, J. Y., Starr, J. L., Schmitz, G., and Fuentes, C. (1990). ''Infiltration under ponded conditions: 3. A predictive equation based on physical parameters.'' *Soil Sci.*, 149(5), 292–300.

Holly, F. M., Jr., and Preissmann, A. (1977). ''Accurate calculation of transport in two dimensions.'' *J. Hydraul. Div., Am. Soc. Civ. Eng.*, 103(11), 1259–1277.

Holly, F. M., Jr., and Toda, K. (1985). ''Hybrid numerical schemes for linear and nonlinear advection.'' *Proc., 21st Congress IAHR*, IAHR, Melbourne, Australia.

Holly, F. M., Jr., and Usseglio-Polatera, J. M. (1984). ''Dispersion simulation in two-dimensional tidal flow.'' *J. Hydraul. Eng.*, 110(7), 905–926.

Hume, I. H. (1993). ''Determination of infiltration characteristics by volume balance for border check basin.'' *Agric. Water Manage.*, 23, 23–39.

Karpik, R. S., and Crockett, S. R. (1997). ''Semi-lagrangian algorithm for two-dimensional advection-diffusion equation on curvilinear coordinate meshes.'' *J. Hydraul. Eng.*, 123(5), 389–401.

Khanna, M., Malano, H. M., Fenton, J. D., and Turral, H. (2003). ''Two-dimensional simulation model for contour basin layouts in southeast Australia. I: Rectangular basins.'' *J. Irrig. Drain. Eng.*, 129(5), 305–316.

Kochavi, E., Segev, R., and Yomdin, Y. (1991). ''Numerical solution of field problems by nonconforming Taylor discretization.'' *Appl. Math. Model.*, 15(March), 152–157.

Kochavi, E., Segev, R., and Yomdin, Y. (1993). ''Modified algorithms for nonconforming Taylor discretization.'' *Comput. Struct.*, 49(6), 969–979.

Komatsu, T., Holly, Jr., F. M., Nakashiki, N., and Ohgushi, K. (1985). ''Numerical calculation of pollutant transport in one and two dimensions.'' *J. Hydrosci. Hydr. Eng.*, 3(2), 15–30.

Komatsu, T., Ohgushi, K., and Asai, K. (1997). ''Refined numerical scheme for advective transport in diffusion simulation.'' *J. Hydraul. Div., Am. Soc. Civ. Eng.*, 123(1), 41–50.

Korn, G. A., and Korn, T. M. (1961). *Mathematical handbook for scientist and engineers*, McGraw–Hill, New York.

Maheshwari, B., and Jayawardarne, N. (1992). ''Infiltration characteristics of some clayey soils measured during border irrigation.'' *Agric. Water Manage.*, 21, 265–279.

Maheshwari, B., and McMahon, T. A. (1992). ''Modeling shallow overland flow in surface irrigation.'' *J. Irrig. Drain. Eng.*, 118(2), 201–217.

Playan, E., Walker, W. R., and Merkley, G. P. (1994a). ''Two-dimensional simulation of basin irrigation. I: Theory.'' *J. Irrig. Drain. Eng.*, 120(5), 837–856.

Playan, E., Walker, W. R., and Merkley, G. P. (1994b). ''Two-dimensional simulation of basin irrigation. II: Applications.'' *J. Irrig. Drain. Eng.*, 120(5), 857–870.

Press, W. H., Teukolsky, S. A., Vetterling, W. T., and Flannery, B. P. (1989). *Numerical recipes, the art of scientific computing (FORTRAN)*, Cambridge University Press, Cambridge, Mass.

Singh, V. (1996). ''Computation of shallow water flow over a porous medium.'' PhD dissertation, Indian Institute of Technology, Kanpur, India.

Sonnemans, P. J. M., de Goey, L. P. H., and Nieuwenhuizen, J. K. (1991). ''Optimal use of a numerical methods for solving differential equations based on Taylor series expansions.'' *Int. J. Numer. Methods Eng.*, 32, 471–499.